

RSSI-based Secure Localization in the Presence of Malicious Nodes in Sensor Networks

Bodhibrata Mukhopadhyay, Seshan Srirangarajan, and Subrat Kar

Abstract

The ability of a sensor node to determine its location in a sensor network is important in many applications. The infrastructure for the location-based services is an easy target for malicious attacks. We address scenarios where malicious node(s) attempt to disrupt, in an uncoordinated or coordinated manner, the localization process of a target node. We propose four techniques for secure localization: weighted least square (WLS), secure weighted least square (SWLS), and ℓ_1 -norm based techniques LN-1 and LN-1E, in a network that includes one or more compromised anchor nodes. WLS and SWLS techniques are shown to offer significant advantage over existing techniques by assigning larger weights to the anchor nodes that are closer to the target node, and by detecting the malicious nodes and eliminating their measurements from the localization process. In a coordinated attack, the localization problem can be posed as a plane fitting problem where the measurements from non-malicious and malicious anchor nodes lie on two different planes. LN-1E technique estimates these two planes and prevents disruption of the localization process. The Cramer-Rao lower bound (CRLB) for the position estimate is also derived. The proposed techniques are shown to provide better localization accuracy than the existing algorithms.

Index Terms

Received signal strength (RSS), uncoordinated attack, coordinated attack, Cramer-Rao lower bound (CRLB), least square (LS), secure localization.

B. Mukhopadhyay, S. Srirangarajan and S. Kar are with the Department of Electrical Engineering, Indian Institute of Technology Delhi, New Delhi, India. S. Srirangarajan and S. Kar are also associated with the Bharti School of Telecommunication Technology and Management, Indian Institute of Technology Delhi. B. Mukhopadhyay is supported through the Visvesvaraya PhD Scheme Fellowship from the Ministry of Electronics and Information Technology (MEITY), Govt. of India. (e-mail: bodhibrata@gmail.com, seshan@ee.iitd.ac.in, subrat@ee.iitd.ac.in).

I. INTRODUCTION

Rapid developments in the field of micro-electronics, integrated circuit fabrication, and embedded software have increased the computational power, lifetime, and sensing capabilities of wireless sensor nodes. A wireless sensor network (WSN) is formed by a collection of authenticated sensor nodes that communicate among themselves and cooperate for a common purpose. These nodes collect data and transmit it to the base station for further processing. As the monitoring area grows larger, the number of sensor nodes in a network increases and it becomes difficult to keep track of the locations of the sensor nodes manually. However, in the absence of accurate location information, the data from the sensors are not very useful. Localization methods based on different techniques have been presented in the literature including those based on optimization [1]–[3], graph [4], [5], game theory [6], least squares [7], [8], and fingerprinting [9], [10].

Localization techniques are broadly divided into two categories: range-based techniques [11]–[14], and range-free techniques [15], [16]. For determining the position of the target node, range-based techniques use the distance between the target node (node whose location is not known at the time of deployment) and the anchors (nodes whose locations are known at the time of deployment), whereas range-free techniques only use the connectivity information between the nodes. Scenarios where location-based services are used include monitoring activities and movement patterns in farm animals [17], metropolitan air quality monitoring [18], monitoring toddlers and elderly persons, tracking goods in the supply chain industry [19], land slide detection [20], and navigation tool for people in places such as shopping malls and airports.

These location-based services are not immune to security threats including cryptographic attacks such as unauthorized access or modification of the information. Attackers can also gain unauthorized access to the infrastructure responsible for carrying out the localization and/or modify the code on the sensor nodes and turn them into malicious nodes (non-cryptographic attacks). A malicious node does not provide correct information required for localization to the target node. Both types of attacks can result in erroneous location estimation of the target nodes. For determining its location, the target node requires certain information from its neighbouring nodes namely, received signal strength information [21], time of flight (for time of arrival (ToA) or time difference of arrival (TDoA)-based techniques), or connectivity (for techniques such as DV-Hop [22]) information. Various types of attacks on localization techniques have been studied

in the literature [23] such as impersonation (malicious node masquerading as an honest node), distance fraud (malicious node reporting information resulting in incorrect distance estimation such as by arbitrarily varying the transmit power level), time fraud (malicious nodes including incorrect time stamp into the packets sent to the target node), and Sybil attack (malicious node claiming multiple identities/locations representing multiple nodes).

A non-malicious node can also seem to behave like a malicious node if the wireless link between this node and the target node is affected. This can happen if the direct path between the anchor and target node is obstructed, or the transmit antenna is damaged resulting in unusual variation in RSSI values. In addition, distance estimation can be affected due to environmental changes as the path loss exponent depends on temperature and humidity [24], [25]. In such scenarios the localization process can be adversely affected. A GPS signal simulator can initiate a GPS spoofing attack by generating incorrect GPS signals to deceive a GPS receiver [26], [27]. Similarly, spoofed radio signals can disrupt the localization process in a WSN.

In this paper, we present four RSSI-based secure localization techniques. We consider the scenario where a target node attempts to localize itself using RSSI values from its neighboring anchor nodes. It is assumed that the anchors transmit at a fixed predefined power level. However, some of the anchor nodes individually or collaboratively change their transmit power without informing the target node in order to disrupt the localization process.

We propose four secure localization techniques: weighted least squares (WLS) [28], secure weighted least squares (SWLS), and ℓ_1 -norm based localization techniques LN-1 and LN-1E for node location estimation in the presence of malicious anchor nodes using RSSI measurements. We consider both uncoordinated and coordinated attacks by malicious node(s) to disrupt the localization process. We present extensive performance evaluation of the proposed techniques and comparison with two existing secure localization methods, Grad-Desc [29] and LMdS [30]. We also derive the Cramer-Rao lower bound (CRLB) on the root mean square error (RMSE) of the position estimate under uncoordinated and coordinated attacks.

The rest of the paper is organized as follows. Section II discusses prior work in the area of secure localization techniques in WSN. Section III presents the problem formulation and Section IV describes the proposed methods for secure localization. The CRLB for uncoordinated and coordinated attack is derived in Section V. Section VI presents the performance evaluation of the proposed techniques under uncoordinated and coordinated attack. Section VII concludes the paper.

Notation: Uppercase bold letters represent matrices and lowercase bold letters represent vectors. $\text{diag}(\cdot)$ represents a diagonal matrix. $\|\cdot\|_1$ and $\|\cdot\|_2$ represent the ℓ_1 -norm and ℓ_2 -norm, respectively. The cardinality of set \mathcal{A} is denoted by $\text{card}(\mathcal{A})$.

II. RELATED WORK

Lazos and Poovendran [31] proposed a secure localization technique, named SEcure Range-independent LOCalization scheme (SeRLoc), in which the target node determines its position by using beacon information transmitted by both benevolent and malicious anchor nodes. SeRLoc was shown to be resilient to wormhole attack, Sybil attack, and compromise of network entities. Liu et al. [32] proposed two range-based localization techniques namely attack-resistant minimum mean square estimation (ARMMSE) and a voting-based scheme. In ARMMSE, malicious anchor nodes are identified by examining the inconsistency among location references indicated by mean square error of estimation. In the voting-based scheme, the network area is divided into a grid and a node votes for a grid cell if the distance of the grid cell to an anchor node is approximately equal to the estimated distance between the target and anchor node. The target node location is estimated as the centroid of the cell with the highest number of votes.

Li et al. [30] considered two robust localization techniques namely, triangulation and RF-based fingerprinting. For triangulation, they proposed an adaptive least squares and least median of squares (LMdS) based location estimation, and for RF fingerprinting they used a median-based distance metric. In LMdS method, anchors are divided into many subsets of identical sizes with each subset estimating the target node location using least squares. The final target node location is given by the least squares location estimate of the subset with the smallest median residue. It was observed that this subset in an attack scenario is least likely to contain malicious nodes. However, it is assumed that the number of malicious nodes is less than 50% of the number of anchor nodes.

Garg et al. [29] proposed an iterative gradient descent technique with inconsistent measurement pruning to achieve accurate localization in the presence of malicious nodes in a WSN. They consider mobile sensor networks where the nodes are mobile and some of them may be compromised and thus transmit false information. Assuming the measurement noise to be Gaussian the likelihood of the measurements is maximized. To account for the possibility of malicious nodes, the cost function is updated at each iteration by eliminating the anchor nodes with large residues from the localization process.

Jha et al. [33] implemented secure localization in WSN using a game theoretic approach. Their proposed technique combines least trimmed square (LTS) and game theoretic aggregation (GTA) algorithms. In the LTS phase, the technique learns the weights for each of the anchor nodes. These weights corresponds to the reputation of the anchor nodes i.e., nodes with lower weights are likely to be compromised and malicious. Robust localization is achieved using GTA by filtering out information from the malicious anchor nodes.

III. SYSTEM MODEL

Consider a network with N anchor nodes whose locations are known, and one or more target nodes whose locations are to be determined. It is assumed that all the anchor nodes are within the communication range of the target node. The nodes are assumed to transmit at a predefined power level. The target node measures RSSI values of the packets received from the anchor nodes and estimates its distance from each of the anchor nodes. Localization techniques allow the target node to estimate its location using the estimated distances and the known locations of the anchor nodes.

Assuming the signal power loss is dominated by path loss which can be modeled using the log-distance model [8]:

$$p^r = p_0 - 10n \log_{10}(d) \quad (1)$$

where p^r is the received power at the target node, p_0 is the transmit power of the anchor node, n is the path loss exponent, and d is the distance between the target and the anchor node.

Let coordinates of the target and N anchor nodes be represented by $\mathbf{t} = [t^x, t^y]^T$ and $\mathbf{a}_i = [a_i^x, a_i^y]^T$ where $i = 1, \dots, N$, respectively. The anchor nodes are assumed to broadcast packets at regular intervals. Let p_{ij}^r represent RSSI value of the j^{th} packet received from the i^{th} anchor node. Using (1) and the RSSI value from the j^{th} packet, the target node computes its distance from the i^{th} anchor node as $d_{ij} = 10^{\frac{(p_0 - p_{ij}^r)}{10n}}$. Next consider that some of the anchor nodes are malicious and attempt to disrupt the localization process. Two types of localization attacks are considered: uncoordinated and coordinated attacks. In an uncoordinated attack, the malicious node(s) act independently and attempt to disrupt the localization process of the target node, whereas in a coordinated attack the malicious nodes coordinate *among themselves* in order to make the target node appear to be located at a location different from its actual location. These attacks are illustrated in Fig. 1 and can be modeled as described next [29], [33].

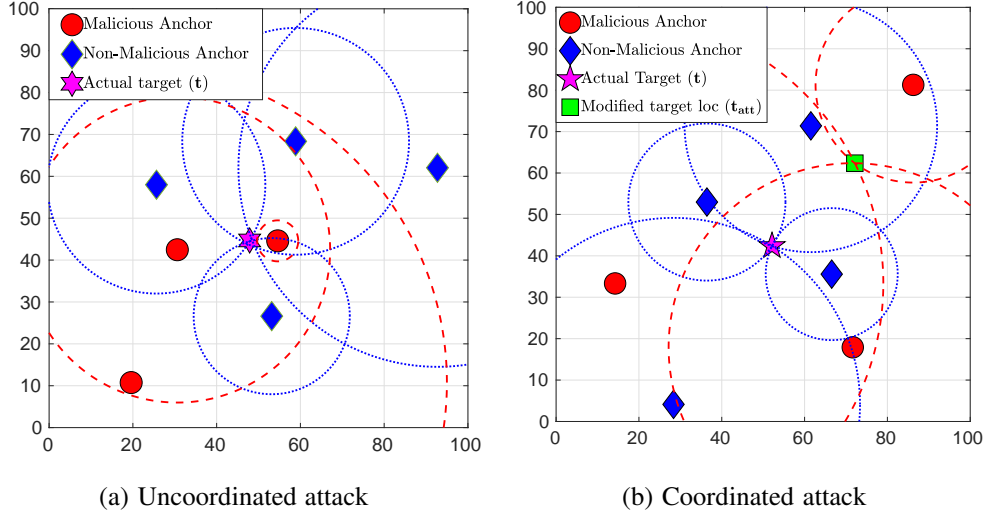


Fig. 1: Attack strategies by malicious anchor nodes in a WSN. The dashed circles represent the estimated distance between the target and malicious anchor nodes, and the dotted circles represent the estimated distance between the target and non-malicious anchor nodes in the absence of measurement noise.

1) *Uncoordinated attack*: We consider non-cryptographic attacks where the malicious nodes change their transmit power levels arbitrarily and do not report it to the target node. This type of attack can be modeled as:

$$p_i^r = \begin{cases} p_0 - 10n \log_{10}(d_i) + \eta & \text{if node } i \text{ is non-malicious} \\ p_{0_i} - 10n \log_{10}(d_i) + \eta & \text{if node } i \text{ is malicious,} \end{cases} \quad (2)$$

where $\eta \sim \mathcal{N}(0, \sigma^2)$ is a Gaussian random variable representing measurement noise, $d_i = \|\mathbf{t} - \mathbf{a}_i\|_2$ is the distance between the i^{th} anchor node located at \mathbf{a}_i and the actual target node located at \mathbf{t} , p_0 is the predefined transmit power of the anchor nodes, p_{0_i} is the transmit power of the i^{th} malicious anchor node, and p_i^r is the received power at the target node from the i^{th} anchor node. Let $p_{0_i} = p_0 + \kappa$ where $\kappa \sim \mathcal{N}(0, \sigma_{\text{att}}^2)$ is a Gaussian random variable with variance σ_{att}^2 representing the uncertainty introduced by the malicious anchor nodes in their transmit power levels to disrupt the localization process.

Fig. 1(a) illustrates an uncoordinated attack where a target node attempts to localize itself using information from 7 anchor nodes of which 3 are malicious. The malicious anchor nodes change their transmit power levels dynamically and since the target node is not aware of their

true transmit power (p_{0_i}), it incorrectly estimates its distance from the malicious anchor nodes resulting in large error in its estimated location.

2) *Coordinated attack*: Coordinated attacks are stronger attacks than the uncoordinated attacks as in coordinated attacks the malicious nodes communicate among themselves with the aim to make the target node appear to be located at a location different from its actual location. It is assumed that the malicious anchor nodes are aware of the actual location of the target node. The coordinated attack can be modeled as:

$$p_i^r = \begin{cases} p_0 - 10n \log_{10}(d_i) + \eta & \text{if node } i \text{ is non-malicious,} \\ p_{0_i}^c - 10n \log_{10}(d_i) + \eta & \text{if node } i \text{ is malicious} \end{cases} \quad (3)$$

where $d_i = \|\mathbf{t} - \mathbf{a}_i\|_2$, $p_{0_i}^c = p_0 - 10n \log_{10}(\chi_i)$ with $\chi_i = \frac{\|\mathbf{t}_{\text{att}} - \mathbf{a}_i\|_2}{\|\mathbf{t} - \mathbf{a}_i\|_2}$. \mathbf{t}_{att} is the location where the malicious anchor nodes are trying to make the target node appear to be located, and $p_{0_i}^c$ is the transmit power of the i^{th} malicious anchor node. Thus, χ_i is the factor by which the malicious anchor nodes scale the actual distance between themselves and the target node.

A coordinated attack is shown in Fig. 1(b) where 3 malicious anchor nodes attempt to make the target node appear to be located at \mathbf{t}_{att} instead of its actual location \mathbf{t} . It is seen that the dashed circles, with radius equal to the erroneous distance between the malicious anchor nodes and the target node, intersect at \mathbf{t}_{att} , whereas the dotted circles with radius equal to the actual distance between the non-malicious anchor nodes and the target node intersect at \mathbf{t} .

IV. PROPOSED TECHNIQUES FOR SECURE LOCALIZATION

The variation in the received power (p^r) as a function of the distance (d) between the anchor and target node is shown in Fig. 2. From (1):

$$d = 10^{\left(\frac{p_0 - p^r}{10n}\right)} \Rightarrow d = c \cdot 10^{\frac{-p^r}{10n}} \quad (4)$$

where $c = 10^{\frac{p_0}{10n}}$. As the relationship between p^r and d is non-linear, variations in the received power affect the estimated distance in a non-linear manner. From Fig. 2, it is seen that the distance estimates are more robust to noise when the anchor nodes are close to the target node than when the anchor nodes are farther from the target node. Thus, anchor nodes closer to the target node should be given a larger weight in the localization process than anchor nodes that are farther.

In Fig. 2, a target node that receives packet with power p_k^r from the k^{th} anchor node is estimated to be at a distance d_k from it. Positive and negative variations in the received power (p_k^r) are

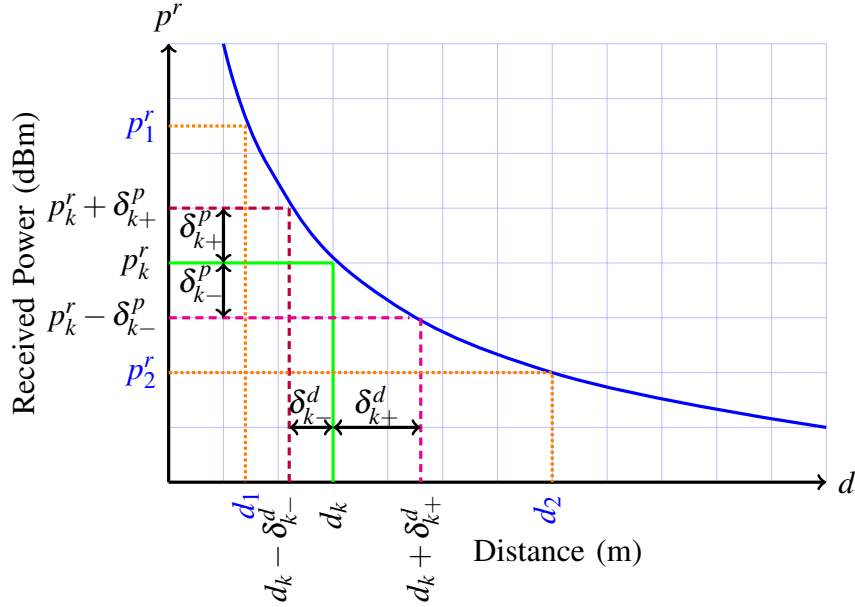


Fig. 2: Effect on distance estimation due to variations in the received power.

represented by δ_{k+}^p and δ_{k-}^p , and the corresponding variation in distance estimates are represented by δ_{k-}^d and δ_{k+}^d . Lemma IV.1 quantifies the variation in the estimated distance corresponding to a variation in the received power.

Lemma IV.1. $\delta_{k-}^d = g(\delta_{k+}^p) 10^{-\frac{p_k^r}{10n}}$ and $\delta_{k+}^d = -g(-\delta_{k-}^p) 10^{-\frac{p_k^r}{10n}}$ where $g(x) = c \left(1 - 10^{-\frac{x}{10n}}\right)$ and $\delta_{k+}^d, \delta_{k-}^d, \delta_{k+}^p, \delta_{k-}^p$ are all positive quantities.

Proof. $d_k - \delta_{k-}^d = c 10^{-\frac{p_k^r + \delta_{k+}^p}{10n}}$, $\delta_{k-}^d = c 10^{-\frac{p_k^r}{10n}} - c 10^{-\frac{p_k^r + \delta_{k+}^p}{10n}} = 10^{-\frac{p_k^r}{10n}} c \left(1 - 10^{-\frac{\delta_{k+}^p}{10n}}\right) = 10^{-\frac{p_k^r}{10n}} g(\delta_{k+}^p)$.

Similarly, $d_k + \delta_{k+}^d = c 10^{-\frac{p_k^r - \delta_{k-}^p}{10n}} \Rightarrow \delta_{k+}^d = -10^{-\frac{p_k^r}{10n}} g(-\delta_{k-}^p)$. \square

Lemma IV.2. For the same amount of variation (δ_k^p) on the received power p_k^r , the received power with negative deviation ($p_k^r - \delta_k^p$) will result in larger variation in the distance estimate than the received power with positive deviation ($p_k^r + \delta_k^p$) i.e., if $\delta_{k+}^p = \delta_{k-}^p = \delta_k^p$, then $\delta_{k+}^d > \delta_{k-}^d$.

Proof. Using Lemma IV.1 it can be shown that

$$g(x) + g(-x) = c \left(2 - 10^{-\frac{x}{10n}} - 10^{\frac{x}{10n}}\right) = - \underbrace{\left(c 10^{-\frac{x}{10n}}\right)}_a \underbrace{\left(10^{\frac{x}{10n}} - 1\right)^2}_b \leq 0 \quad (5)$$

$g(x) + g(-x)$ is always negative because a and b are always positive for all $x \in \mathbb{R}$.

The variation in distance corresponding to the negative and positive change in received power p_k^r are given by $d_k + \delta_{k+}^d$ and $d_k - \delta_{k-}^d$, respectively. From Lemma IV.1:

$$\delta_{k+}^d = -g(-\delta_k^p)10^{\frac{p_k^r}{10n}} \text{ and } \delta_{k-}^d = g(\delta_k^p)10^{\frac{p_k^r}{10n}} \quad (6)$$

Using (5) and (6), it is seen that $\delta_{k+}^d \geq \delta_{k-}^d$ when $\delta_{k+}^p = \delta_{k-}^p = \delta_k^p$ (refer Fig. 2). \square

Lemma IV.3 states that the distance estimation using RSSI values from anchor nodes that are farther from the target node is less robust to variation in the received power.

Lemma IV.3. *For the same amount of variation at two different received power levels, the lower received power level will result in larger variation in the distance estimate than the higher received power level i.e., if $p_1^r > p_2^r$ and $\delta_1^p = \delta_2^p$, then $\delta_2^d > \delta_1^d$.*

Proof. If variation in the received power levels is positive i.e., $p_1^r + \delta_1^p$ and $p_2^r + \delta_2^p$ where $\delta_1^p = \delta_2^p$, then the relationship between the corresponding variations in distance estimates is $\delta_2^d > \delta_1^d$. Using Lemma IV.1:

$$p_1^r > p_2^r \Rightarrow g(\delta_2^p)10^{\frac{-p_2^r}{10n}} > g(\delta_1^p)10^{\frac{-p_1^r}{10n}} \Rightarrow \delta_2^d > \delta_1^d \quad (7)$$

This relationship also holds if the variation in the received power levels is negative. \square

From Lemma IV.3, we can say that the malicious nodes that are closer to the target node can have a greater impact in disrupting the localization process than nodes that are farther. To reduce the effect of the malicious anchor nodes we next propose secure localization techniques.

A. Weighted Least Square (WLS)

We propose a secure localization technique based on the weighted least squares algorithm [28]. This is a modified version of the least squares [7] where the anchor nodes are assigned weights based on their distance from the target node. The target receives P packets from each of the anchor nodes and computes the mean received power as $\overline{p_i^r} = \frac{1}{P} \sum_{j=1}^P p_{ij}^r$.

Using $\overline{p_i^r}$, the target node estimates its distance from the i^{th} anchor node as $\overline{d_i}$. Given \mathbf{a}_i and $\overline{d_i}$ for $i = 1, \dots, N$, the target node position estimation can be formulated as a weighted least squares problem where each of the distance estimates is weighted by the variance of $\overline{d_i}^2$. Assuming the distance estimate to be a random variable, its cumulative distribution function (CDF) is:

$$P(d_i \leq \gamma) = P\left(\frac{\eta}{\sigma} \leq \frac{p_i^r - p_0 + 10n \log_{10} \gamma}{\sigma}\right) = 1 - Q(f(\gamma))$$

where $Q(\cdot)$ is the Q-function and $f(\gamma) = \frac{10n}{\sigma} \log_{10} \left(\frac{\gamma}{d_i} \right)$. The probability density function (PDF) of d_i can be shown to be:

$$f_{d_i}(\gamma) = \frac{5n}{\gamma\sigma \ln(10)} \sqrt{\frac{2}{\pi}} \exp \left(-\frac{50n^2 \ln^2 \left(\frac{\gamma}{d_i} \right)}{\sigma^2 \ln^2(10)} \right) \quad (8)$$

Using (8), the variance of d_i and d_i^2 can be shown to be:

$$f_{d_i}^{\text{Var}}(d_i, \sigma) = d_i^2 \exp \left(\frac{\sigma^2}{18.86n^2} \right) \left[\exp \left(\frac{\sigma^2}{18.86n^2} \right) - 1 \right] \quad (9)$$

$$f_{d_i^2}^{\text{Var}}(d_i, \sigma) = d_i^4 \exp \left(\frac{\sigma^2}{4.715n^2} \right) \left[\exp \left(\frac{\sigma^2}{4.715n^2} \right) - 1 \right] \quad (10)$$

The measurement matrix \mathbf{P}^r ($= [p_{ij}^r]$ where $i = 1, \dots, N$ and $j = 1, \dots, P$) consists of the RSSI values of the P packets received by the target node from each of the N anchor nodes (both malicious and non-malicious nodes). Consider a diagonal weighing matrix W whose elements are inverse of the variance of d_i^2 . The measurement model can be expressed as $\mathbf{A}\mathbf{t} + \boldsymbol{\varepsilon} = \mathbf{b}$ where \mathbf{A} and \mathbf{b} are given in terms of the anchor node positions (\mathbf{a}_i) and distance estimates (\bar{d}_i) as:

$$\mathbf{A} = \begin{pmatrix} -2a_1^x & -2a_1^y & 1 \\ -2a_2^x & -2a_2^y & 1 \\ \vdots & \vdots & \vdots \\ -2a_N^x & -2a_N^y & 1 \end{pmatrix}, \mathbf{b} = \begin{pmatrix} \bar{d}_1^2 - (a_1^x)^2 - (a_1^y)^2 \\ \bar{d}_2^2 - (a_2^x)^2 - (a_2^y)^2 \\ \vdots \\ \bar{d}_N^2 - (a_N^x)^2 - (a_N^y)^2 \end{pmatrix} \quad (11)$$

Assuming the measurement noise $\boldsymbol{\varepsilon}$ to be Gaussian distributed, estimation of the target node position can be formulated as a weighted least squares problem and Algorithm 1 presents the WLS secure localization technique.

B. Secure Weighted Least Square (SWLS)

Consider an uncoordinated attack scenario where the malicious nodes change their transmit powers arbitrarily without communicating this to the target node (refer Section III-1). The received power (p_{0_i}) from a malicious anchor node can be expressed using (2) as:

$$p_i^r = p_0 - 10n \log_{10}(d_i) + \eta + \kappa \quad (12)$$

Thus, the RSSI values from the malicious and non-malicious anchor nodes have standard deviation of $\sqrt{\sigma^2 + \sigma_{\text{att}}^2}$ and σ , respectively. SWLS attempts to identify the malicious anchor nodes by observing the RSSI values, and eliminates them from the localization process. The detailed procedure of the SWLS localization is given in Algorithm 2. Let \mathbf{D} be the $P \times N$ matrix

Algorithm 1 WLS Localization

Input: \mathbf{P}^r , \mathbf{a}_i ($i = 1, \dots, N$), σ
Output: $\hat{\mathbf{t}} = [t^x, t^y]^T$
Initialize: \mathbf{A} , \mathbf{b}

- 1: $\bar{\mathbf{p}}^r = \frac{1}{P} \left[\sum_{j=1}^P p_{1j}^r, \sum_{j=1}^P p_{2j}^r, \dots, \sum_{j=1}^P p_{Nj}^r \right]^T$
 - 2: $\bar{\mathbf{d}} = [\bar{d}_1, \bar{d}_2, \dots, \bar{d}_N]^T = 10^{\frac{(p_0 - \bar{\mathbf{p}}^r)}{10n}}$
 - 3: $\sigma_{d^2}^2(i) = f_{d^2}^{\text{Var}}(\bar{d}_i, \sigma)$, $i = 1, \dots, N$ (using (10))
 - 4: $\mathbf{W} = \text{diag}\left(1/\sigma_{d^2}^2(1), 1/\sigma_{d^2}^2(2), \dots, 1/\sigma_{d^2}^2(N)\right)$
 - 5: $\hat{\mathbf{q}} = (\mathbf{A}^T \mathbf{W} \mathbf{A})^{-1} \mathbf{A}^T \mathbf{W} \mathbf{b}$
 - 6: $\hat{\mathbf{t}} = [\hat{q}_1, \hat{q}_2]^T$
-

Algorithm 2 SWLS Localization

Input: \mathbf{P}^r , \mathbf{a}_i ($i = 1, \dots, N$), σ , ζ
Output: $\hat{\mathbf{t}} = [t^x, t^y]^T$
Initialize: \mathbf{A} , \mathbf{b} , $\mathcal{M} = \emptyset$

- 1: $\mathbf{D} = 10^{\frac{p_0 - \mathbf{P}^r}{10n}}$
 - 2: $\bar{\mathbf{p}}^r = \frac{1}{P} \left[\sum_{j=1}^P p_{1j}^r, \sum_{j=1}^P p_{2j}^r, \dots, \sum_{j=1}^P p_{Nj}^r \right]^T$
 - 3: $\bar{\mathbf{d}} = 10^{\frac{p_0 - \bar{\mathbf{p}}^r}{10n}} = [\bar{d}_1, \bar{d}_2, \dots, \bar{d}_N]^T$
 - 4: **for** $i = 1$ to N **do**
 - 5: $\hat{\sigma}_{\text{est}} = \arg \min_{\sigma_{\text{est}} \geq 0} |\text{Var}(d_{i1}, d_{i2}, \dots, d_{iP}) - f_d^{\text{Var}}(\bar{d}_i, \sigma_{\text{est}})|$, using (13)
 - 6: $\mathcal{M} = \mathcal{M} \cup \{i \mid \hat{\sigma}_{\text{est}} < \zeta \sigma\}$ (index of non-malicious nodes)
 - 7: **end for**
 - 8: $\sigma_{d^2}^2(k) = f_{d^2}^{\text{Var}}(\bar{\mathbf{d}}_k, \sigma)$ where $k \in \mathcal{M}$, using (10)
 - 9: $\hat{\mathbf{A}} = \mathbf{A}(j, :)$, $\hat{\mathbf{b}} = \mathbf{b}(j, :)$, $j \in \mathcal{M}$
 - 10: $\mathbf{W} = \text{diag}(1/\sigma_{d^2}^2(1), 1/\sigma_{d^2}^2(2), \dots, 1/\sigma_{d^2}^2(\text{card}(\mathcal{M})))$
 - 11: $\hat{\mathbf{q}} = (\hat{\mathbf{A}}^T \mathbf{W} \hat{\mathbf{A}})^{-1} \hat{\mathbf{A}}^T \mathbf{W} \hat{\mathbf{b}}$
 - 12: $\hat{\mathbf{t}} = [\hat{q}_1, \hat{q}_2]^T$
-

of distance estimates from the target node to each of the anchor nodes i.e., $\mathbf{D} = [d_{ij}]$ where $i = 1, \dots, N$ and $j = 1, \dots, P$, computed using (4). The average distance (\bar{d}_i) between the target node and an anchor node is calculated using \bar{p}^r obtained from the RSSI values of P packets and not as a column average of the matrix \mathbf{D} . This is due to the fact that the estimated distances (d_i) do not follow a Gaussian distribution (refer (8)).

Variance of the distance estimates is calculated based on the estimated distances from each of the P packets and using (9) for different values of the noise standard deviation. An estimate of the noise standard deviation (σ_{est}) is obtained for each of the anchor nodes by minimizing $|\text{Var}(d_{i1}, d_{i2}, \dots, d_{iP}) - f_d^{\text{var}}(\bar{d}_i, \sigma_{\text{est}})|$ where $\text{Var}(d_{i1}, d_{i2}, \dots, d_{iP})$ represents the variance of the distance estimates calculated from each of the P packets. The malicious nodes are identified by applying a threshold on $\hat{\sigma}_{\text{est}}$ with the threshold level set to $\zeta \sigma$ where $\zeta > 0$. Finally, weighted least square localization (as discussed in Algorithm 1) is applied by considering only the non-malicious anchor nodes. The closed-form solution of the estimate $\hat{\sigma}_{\text{est}}$ is given by (used in line 5 of Algorithm 2):

$$\hat{\sigma}_{\text{est}} = \sqrt{18.86n^2 \ln \left(0.5 + 0.5 \sqrt{1 + \frac{4\text{Var}(d_{i1}, d_{i2}, \dots, d_{iP})}{\bar{d}_i^2}} \right)} \quad (13)$$

The derivation of (13) is provided in the Appendix A.

This technique relies on the variance in the RSSI values, and in the case of a coordinated attack the variance remains the same for malicious and non-malicious nodes (refer (3)). Thus, this technique is not robust to coordinated attacks on the localization process.

C. Localization using ℓ_1 -norm Optimization

The localization problem can be posed as a 3-dimensional plane fitting problem $z = f(x, y)$ where z represents \mathbf{b} , and x, y represent the first two columns of \mathbf{A} (refer (11)). The objective is to find a plane $z = \alpha x + \beta y + \gamma$ where $\alpha = t^x$, $\beta = t^y$, and $\gamma = (t^x)^2 + (t^y)^2$, that fits the measurements (or data points) $\langle -2\alpha_i^x, -2\alpha_i^y, \bar{d}_i^2 - (\alpha_i^x)^2 - (\alpha_i^y)^2 \rangle$, $i = 1, \dots, N$. The values of α , β , and γ can be obtained by minimizing the ℓ_2 -norm based distance between the measurements and the plane:

$$\begin{aligned} \min_{\mathbf{u}} \quad & \|\mathbf{r}\|_2^2 \\ \text{subject to} \quad & \mathbf{r} = \mathbf{A}\mathbf{u} - \mathbf{b} \end{aligned} \quad (14)$$

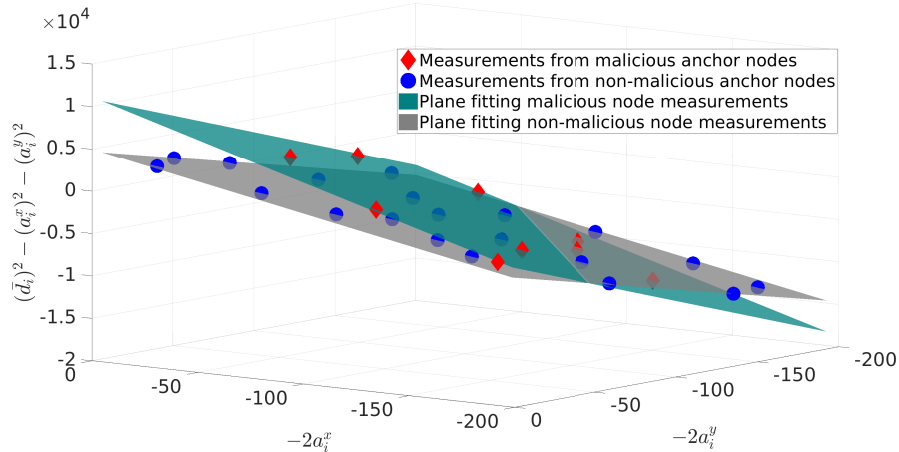


Fig. 3: Planes containing measurements corresponding to the malicious and non-malicious anchor nodes. Anchor nodes are randomly distributed with 31% of the anchor nodes being malicious, measurement noise (σ) is 0 dB, and $\|\mathbf{t} - \mathbf{t}_{\text{att}}\|_2 = 35.35$ m.

where $\mathbf{u} = [\alpha, \beta, \gamma]^T$. The closed form solution of (14) is $\mathbf{u} = \mathbf{A}^\dagger \mathbf{b}$ [34] where \dagger represents the pseudo inverse. This is similar to the localization process discussed in Algorithm 1.

In an uncoordinated attack scenario, the measurements representing points in three dimensions are divided into two categories on the basis of the variance in the received power. Measurements from non-malicious nodes display less variance than those from malicious nodes. From a curve fitting perspective, the data points corresponding to the malicious nodes can be treated as outliers. However, in a coordinated attack, measurements from all the nodes display similar variance since the malicious nodes do not vary their transmit power randomly (refer (3)). The transmit power of the malicious anchor nodes is assumed to be different from those of the non-malicious anchor nodes, and depends on the value of χ_i . Fig. 3 shows a coordinated attack visualized as a plane fitting problem. The data points corresponding to the measurements from malicious and non-malicious anchor nodes are shown to lie on two different planes. Determining these planes will enable us to estimate the location of the target node (\mathbf{t}) and the location where the malicious anchor nodes intend to make the target node appear to be located (\mathbf{t}_{att}). As $\|\mathbf{t} - \mathbf{t}_{\text{att}}\|_2$ increases the measurements corresponding to the malicious anchor nodes move farther from the plane that fits the measurements from non-malicious anchor nodes.

In a coordinated attack scenario, measurements from the malicious anchor nodes can thus be treated as outliers. Hence, under both uncoordinated and coordinated attacks, the optimization

problem (14) can be rewritten as a robust plane fitting problem by replacing the ℓ_2 -norm in the objective with an ℓ_1 -norm [34], [35]:

$$\begin{aligned} \min_{\mathbf{u}} \quad & \|\mathbf{r}\|_1 \\ \text{subject to} \quad & \mathbf{r} = \mathbf{A}\mathbf{u} - \mathbf{b} \end{aligned} \quad (15)$$

(15) can be solved efficiently using ADMM [36] by reformulating it as:

$$\begin{aligned} \min_{\mathbf{u}, \mathbf{z}} \quad & \|\mathbf{z}\|_1 \\ \text{subject to} \quad & \mathbf{A}\mathbf{u} - \mathbf{z} = \mathbf{b} \end{aligned} \quad (16)$$

Using the standard ADMM steps, (16) can be solved iteratively as:

$$\mathbf{u}^{k+1} = \mathbf{G}\mathbf{A}^T \left(\mathbf{b} + \mathbf{z}^k - \frac{\mathbf{y}^k}{\rho} \right) \quad (16a)$$

$$\mathbf{z}^{k+1} = S_{\frac{1}{\rho}} \left(\mathbf{A}\mathbf{u}^{k+1} - \mathbf{b} + \frac{\mathbf{y}^k}{\rho} \right) \quad (16b)$$

$$\mathbf{y}^{k+1} = \mathbf{y}^k + \rho \left(\mathbf{A}\mathbf{u}^{k+1} - \mathbf{z}^{k+1} - \mathbf{b} \right) \quad (16c)$$

where $\mathbf{G} = (\mathbf{A}^T\mathbf{A})^{-1}$, \mathbf{y} is the dual variable (Lagrange multiplier), and $\rho (> 0)$ is the penalty parameter for the violation of the linear constraint [37]. $S_{\frac{1}{\rho}}(x) = \left\{ \max \left(|x| - \frac{1}{\rho}, 0 \right) \cdot \text{sign}(x) \right\}$ is the proximal operator of ℓ_1 [38]. The convergence criteria for solving (16) using ADMM is $|\|\mathbf{z}^{k+1}\|_1 - \|\mathbf{z}^k\|_1| \leq \text{Conv}_{\text{ADMM}}$, where $\text{Conv}_{\text{ADMM}} > 0$.

We propose two localization techniques LN-1 and LN-1E. LN-1 attempts to solve the optimization problem (16) in order to localize the target node in both uncoordinated and coordinated attack scenarios. LN-1E is an improvement over LN-1 to handle only coordinated attacks. LN-1E identifies the malicious anchor nodes by applying LN-1 and then recomputes the plane by solving (16) after eliminating the measurements corresponding to the malicious anchor nodes. Using LN-1, we determine the ‘‘best fitting’’ plane for the measurements from all the anchor nodes $\hat{f}(x, y) = \hat{\alpha}x + \hat{\beta}y + \hat{\gamma}$. It is found that the data points corresponding to the non-malicious anchor nodes are closer to this plane than those corresponding to the malicious anchor nodes. K-means clustering [39] is used to partition the anchor nodes into two groups based on their distance from this plane. The steps for implementing LN-1 and LN-1E are listed in Algorithm 3. The node-to-plane distances are grouped into two clusters using the K-means clustering algorithm, and the centroid of the cluster containing the malicious nodes is always farther from the plane than the centroid of the other cluster. After identifying the two clusters,

we recompute the “best fitting” plane for the measurements only from the non-malicious anchor nodes as $\hat{f}_{\text{new}}(x, y) = \hat{\alpha}_{\text{new}}x + \hat{\beta}_{\text{new}}y + \hat{\gamma}_{\text{new}}$.

Algorithm 3 LN-1 and LN-1E Localization

Input: \mathbf{A} , \mathbf{b} , N

Output: Estimated target locations $\hat{\mathbf{t}}_{LN1}$, $\hat{\mathbf{t}}_{LN1E}$

Computing the “best fitting” plane using measurements from all the anchor nodes:

- 1: $\hat{\mathbf{u}} = [\hat{\alpha} \ \hat{\beta} \ \hat{\gamma}]^T$ by solving (16)
 - 2: $\hat{f}(x, y) = \hat{\alpha}x + \hat{\beta}y + \hat{\gamma}$
 - 3: $\hat{\mathbf{t}}_{LN1} = [\hat{\alpha} \ \hat{\beta}]^T$
 - 4: Compute distances d_i^p of the data points $\langle -2a_i^x, -2a_i^y, \bar{d}_i^2 - (a_i^x)^2 - (a_i^y)^2 \rangle$ from the plane $\hat{f}(x, y)$, $i = 1, \dots, N$.
 - 5: Using K-means algorithm, group the distances d_i^p into two clusters. The cluster closer to the plane $\hat{f}(x, y)$ is assumed to represent the non-malicious anchor nodes.
 - 6: $\hat{f}_{\text{new}}(x, y) = \hat{\alpha}_{\text{new}}x + \hat{\beta}_{\text{new}}y + \hat{\gamma}_{\text{new}}$, using only measurements from non-malicious anchor nodes.
 - 7: $\hat{\mathbf{u}}_{\text{new}} = [\hat{\alpha}_{\text{new}} \ \hat{\beta}_{\text{new}} \ \hat{\gamma}_{\text{new}}]^T$ by solving (16)
 - 8: $\hat{\mathbf{t}}_{LN1E} = [\hat{\alpha}_{\text{new}} \ \hat{\beta}_{\text{new}}]^T$
-

Remark. The identification of malicious anchor nodes will also enable determining the location \mathbf{t}_{att} where the malicious nodes intend to make the target appear to be located. This can be useful from a security perspective in many applications and will be explored as part of future work.

V. CRAMER-RAO LOWER BOUND (CRLB)

CRLB provides a lower bound on the variance of an unbiased estimator and can be used as a benchmark for other estimators [7], [40]. The mean square error (MSE) of an unbiased estimator ($\hat{\mathbf{t}}$) of the target node position (\mathbf{t}) can be expressed as shown below and bounded using the CRLB as:

$$\text{MSE}(\hat{\mathbf{t}}) = \mathbb{E} \left[(\hat{t}^x - t^x)^2 \right] + \mathbb{E} \left[(\hat{t}^y - t^y)^2 \right] = \text{Var}(\hat{t}^x) + \text{Var}(\hat{t}^y) \geq [\mathbf{F}^{-1}]_{11} + [\mathbf{F}^{-1}]_{22} = \text{tr}(\mathbf{F}^{-1})$$

where \mathbf{F} is the Fisher information matrix (FIM). The RMSE of an unbiased estimator satisfies $\text{RMSE}(\hat{\mathbf{t}}) \geq \sqrt{\text{tr}(\mathbf{F}^{-1})}$. Thus, the CRLB provides a lower bound on the RMSE of unbiased estimators for estimating the target node position.

For computing the CRLB, we assume that the identity of malicious and non-malicious anchor nodes is known. In addition, σ and σ_{att} are assumed to be known. We define \mathcal{A}_{nm} and \mathcal{A}_{m} as sets containing the indices of non-malicious and malicious anchor nodes, respectively.

A. CRLB for Uncoordinated Attack

The probability density function (PDF) of the received signal power at the target node in an uncoordinated attack can be expressed as:

$$p(\mathbf{P}^r; \mathbf{t}) = \prod_{j=1}^P \left[\prod_{i \in \mathcal{A}_{\text{nm}}} \frac{1}{\sqrt{2\pi\sigma^2}} \exp \frac{-\left(p_{ij}^r - p_0 + 10n \log_{10}(d_i)\right)^2}{2\sigma^2} \right. \\ \left. \times \prod_{k \in \mathcal{A}_{\text{m}}} \frac{1}{\sqrt{2\pi\sigma_{\text{eff}}^2}} \exp \frac{-\left(p_{kj}^r - p_0 + 10n \log_{10}(d_k)\right)^2}{2\sigma_{\text{eff}}^2} \right] \quad (17)$$

where $\sigma_{\text{eff}}^2 = \sigma^2 + \sigma_{\text{att}}^2$. The PDF $p(\mathbf{P}^r; \mathbf{t})$ satisfies the regularity conditions $\mathbb{E} \left[\frac{\partial \ln(p(\mathbf{P}^r; \mathbf{t}))}{\partial t^x} \right] = 0$ and $\mathbb{E} \left[\frac{\partial \ln(p(\mathbf{P}^r; \mathbf{t}))}{\partial t^y} \right] = 0$, and therefore, the CRLB is given by $t_{\text{CRLB}}^{\text{uc}} = \sqrt{\text{tr}(\mathbf{F}_{\text{uc}}^{-1})}$ where the FIM is given by $\mathbf{F}_{\text{uc}} = [f_{xx}^{\text{uc}} \ f_{xy}^{\text{uc}}; f_{yx}^{\text{uc}} \ f_{yy}^{\text{uc}}]$ where:

$$f_{xx}^{\text{uc}} = \frac{100Pn^2}{\ln^2(10)} \left[\frac{1}{\sigma^2} \sum_{i \in \mathcal{A}_{\text{nm}}} \frac{(a_i^x - t^x)^2}{\|\mathbf{a}_i - \mathbf{t}\|_2^4} + \frac{1}{\sigma_{\text{eff}}^2} \sum_{k \in \mathcal{A}_{\text{m}}} \frac{(a_k^x - t^x)^2}{\|\mathbf{a}_k - \mathbf{t}\|_2^4} \right] \\ f_{yy}^{\text{uc}} = \frac{100Pn^2}{\ln^2(10)} \left[\frac{1}{\sigma^2} \sum_{i \in \mathcal{A}_{\text{nm}}} \frac{(a_i^y - t^y)^2}{\|\mathbf{a}_i - \mathbf{t}\|_2^4} + \frac{1}{\sigma_{\text{eff}}^2} \sum_{k \in \mathcal{A}_{\text{m}}} \frac{(a_k^y - t^y)^2}{\|\mathbf{a}_k - \mathbf{t}\|_2^4} \right] \quad (18) \\ f_{xy}^{\text{uc}} = \frac{100Pn^2}{\ln^2(10)} \left[\frac{1}{\sigma^2} \sum_{i \in \mathcal{A}_{\text{nm}}} \frac{(a_i^x - t^x)(a_i^y - t^y)}{\|\mathbf{a}_i - \mathbf{t}\|_2^4} + \frac{1}{\sigma_{\text{eff}}^2} \sum_{k \in \mathcal{A}_{\text{m}}} \frac{(a_k^x - t^x)(a_k^y - t^y)}{\|\mathbf{a}_k - \mathbf{t}\|_2^4} \right]$$

B. CRLB for Coordinated Attack

The PDF of the measurement matrix \mathbf{P}^r in a coordinated attack can be expressed as:

$$p(\mathbf{P}^r; \mathbf{t}) = \frac{1}{\sqrt{2\pi\sigma^2}} \prod_{j=1}^P \left[\prod_{i \in \mathcal{A}_{\text{nm}}} \exp \frac{-\left(p_{ij}^r - p_0 + 10n \log_{10}(d_i)\right)^2}{2\sigma^2} \prod_{k \in \mathcal{A}_{\text{m}}} \exp \frac{-\left(p_{kj}^r - p_0 + 10n \log_{10}(d'_k)\right)^2}{2\sigma^2} \right]$$

TABLE I
Different localization techniques being compared.

| Algorithm | Description | Uncoordinated | Coordinated |
|-----------|---|---------------|-------------|
| LS | Least Square based localization [41] | ✓ | ✗ |
| Grad-Desc | Iterative gradient descent with selective pruning [29] | ✓ | ✓ |
| LMdS | Least Median Square [30] | ✓ | ✓ |
| WLS | Weighted LS | ✓ | ✓ |
| SWLS | Secure Weighted LS | ✓ | ✗ |
| LN-1 | ℓ_1 -Norm based | ✓ | ✓ |
| LN-1E | ℓ_1 -Norm based with malicious anchor node elimination | ✗ | ✓ |
| ML | ML estimator (20), initialized with true target node location | ✓ | ✗ |

where $d'_k = \|\mathbf{a}_k - \mathbf{t}_{\text{att}}\|_2$. The PDF $p(\mathbf{P}^r; \mathbf{t})$ satisfies the regularity conditions $\mathbb{E} \left[\frac{\partial \ln(p(\mathbf{P}^r; \mathbf{t}))}{\partial t^x} \right] = 0$ and $\mathbb{E} \left[\frac{\partial \ln(p(\mathbf{P}^r; \mathbf{t}))}{\partial t^y} \right] = 0$, and therefore the CRLB in the coordinated attack is $t_{\text{CRLB}}^c = \sqrt{\text{tr}(\mathbf{F}_c^{-1})}$.

The FIM for coordinated attack is given by $\mathbf{F}_c = [f_{xx}^c \ f_{xy}^c; f_{yx}^c \ f_{yy}^c]$ where:

$$\begin{aligned}
 f_{xx}^c &= \frac{100Pn^2}{\sigma^2 \ln^2(10)} \left[\sum_{i \in \mathcal{A}_{\text{nm}}} \frac{(a_i^x - t^x)^2}{\|\mathbf{a}_i - \mathbf{t}\|_2^4} + \sum_{k \in \mathcal{A}_m} \frac{(a_k^x - t_{\text{att}}^x)^2}{\|\mathbf{a}_k - \mathbf{t}_{\text{att}}\|_2^4} \right] \\
 f_{yy}^c &= \frac{100Pn^2}{\sigma^2 \ln^2(10)} \left[\sum_{i \in \mathcal{A}_{\text{nm}}} \frac{(a_i^y - t^y)^2}{\|\mathbf{a}_i - \mathbf{t}\|_2^4} + \sum_{k \in \mathcal{A}_m} \frac{(a_k^y - t_{\text{att}}^y)^2}{\|\mathbf{a}_k - \mathbf{t}_{\text{att}}\|_2^4} \right] \\
 f_{xy}^c &= \frac{100Pn^2}{\sigma^2 \ln^2(10)} \left[\sum_{i \in \mathcal{A}_{\text{nm}}} \frac{(a_i^x - t^x)(a_i^y - t^y)}{\|\mathbf{a}_i - \mathbf{t}\|_2^4} + \sum_{k \in \mathcal{A}_m} \frac{(a_k^x - t_{\text{att}}^x)(a_k^y - t_{\text{att}}^y)}{\|\mathbf{a}_k - \mathbf{t}_{\text{att}}\|_2^4} \right]
 \end{aligned} \tag{19}$$

The estimators discussed in this paper (refer Table I) are biased (determined via simulation) and thus the CRLB cannot be used to lower bound their performance. However, the CRLB is used as a benchmark as it represents the minimum RMSE that can be achieved by an unbiased estimator.

VI. PERFORMANCE EVALUATION

We have carried out extensive performance evaluation of the proposed secure localization techniques and compared it with four existing techniques from the literature, namely least squares (LS) [7], LMdS [30], gradient descent (Grad-Desc) [29], [42], and maximum likelihood (ML) [7] methods. We consider a network spread over a $100 \text{ m} \times 100 \text{ m}$ area with 29 anchor nodes and one target node. Anchor nodes are set to transmit at -10 dBm (p_0), and the path loss exponent (n) is assumed to be 4 representing a suburban environment [43].

The LS method solves for the target node location as $\hat{\mathbf{t}} = (\mathbf{A}^T \mathbf{A})^{-1} \mathbf{A}^T \mathbf{b}$. ML estimate for the target node location is obtained by solving the non-convex optimization problem:

$$\hat{\mathbf{t}} = \underset{\mathbf{t}}{\operatorname{argmin}} \sum_{i=1}^N \sum_{j=1}^P (p_{ij}^r - p_0 + 10n \log_{10}(d_i))^2 \quad (20)$$

We solve (20) using the *fminunc* function in Matlab which is based on the quasi-Newton method [44]. ML is initialized with the true location of the target node. For LMdS, we consider 20 (intersecting) subsets with each subset consisting of 4 anchor nodes. For Grad-Desc, the maximum number of iterations is 200 and a constant step size of 0.4 is chosen. Variable step size is not considered as its performance is reported to be similar to that with a constant step size [29]. The threshold for the anchor selection or pruning step in Grad-Desc is empirically set to a value that gives the best performance. In SWLS, ζ is empirically set to 1.5. LN-1 and LN-1E use ADMM to solve (16), and the value of $Conv_{ADMM}$ and ρ are determined empirically and set to 10^{-6} and 0.2, respectively. The maximum number of iterations for allowing ADMM to converge is set to 5000. All results reported in this paper are based on 5000 Monte Carlo simulations.

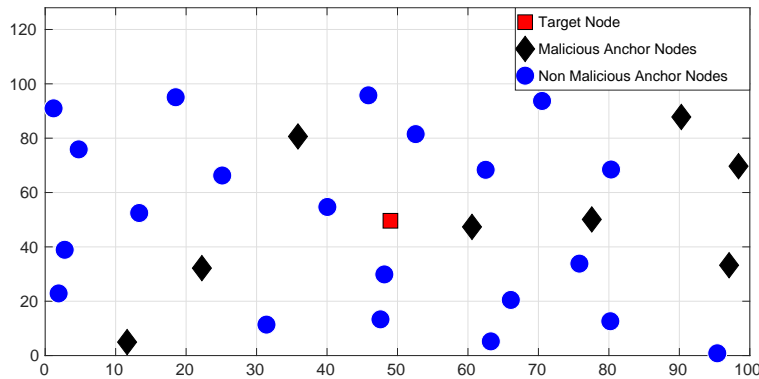
A. Uncoordinated Attack

Fig. 4(a) shows a randomly deployed network with 29 anchor nodes and one target node. The network is assumed to contain 8 malicious anchor nodes (i.e., roughly 28% of the anchor nodes are malicious) which attempt to disrupt the target node's localization process via uncoordinated attack. Fig. 4(b) and Fig. 4(c) show the performance of the various secure localization techniques in terms of the RMS localization error. The RMS localization error is shown as a function of σ_{att} . The target node estimates its position by executing the localization process after receiving 10 packets from each of the anchor nodes. In the Monte Carlo simulations, the topology and the percentage of malicious anchor nodes are kept fixed, while the malicious anchor nodes are chosen randomly from the 29 anchor nodes for each simulation run. Simulations are also carried out to study the performance of the algorithms as the target node moves closer to the edge of the network (refer Fig. 4(c)).

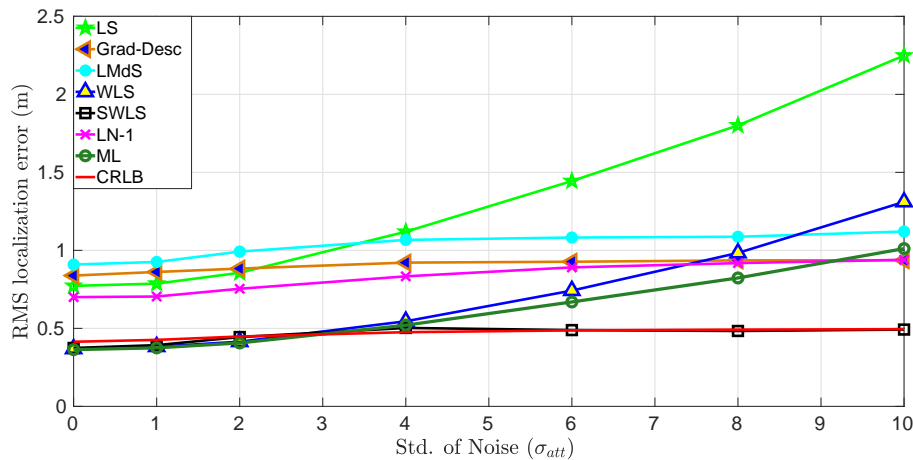
SWLS and WLS techniques assign large weights to the anchor nodes located closer to the target node and thus reduce the effect of the larger distance estimation errors from the farther anchor nodes in the localization process. The performance of SWLS and WLS are similar as long as σ_{att} is not significantly higher than the measurement noise (σ). However, WLS

performance deteriorates as σ_{att} becomes higher than σ and WLS starts assigning larger weight to the malicious anchor nodes which are close to the target node. On the other hand, SWLS outperforms the other techniques as it attempts to eliminate the malicious anchor nodes from the localization process. SWLS is the only estimator whose RMS localization error is closest to the CRLB in most of the scenarios. CRLB is barely affected with the increase in the value of σ_{att} as only 28% of the anchor nodes are malicious. From (18), it can be seen that the CRLB will be significantly effected when the percentage of malicious anchor nodes is higher and σ_{att} is greater than σ . When the target node is moved closer to the edge of the network (refer Fig. 4(c)), the performance of Grad-Desc degrades significantly as the gradient descent algorithm appears to get stuck in a local minima. The relative performance of the other techniques is similar to the case when the target node was located at the center of the network.

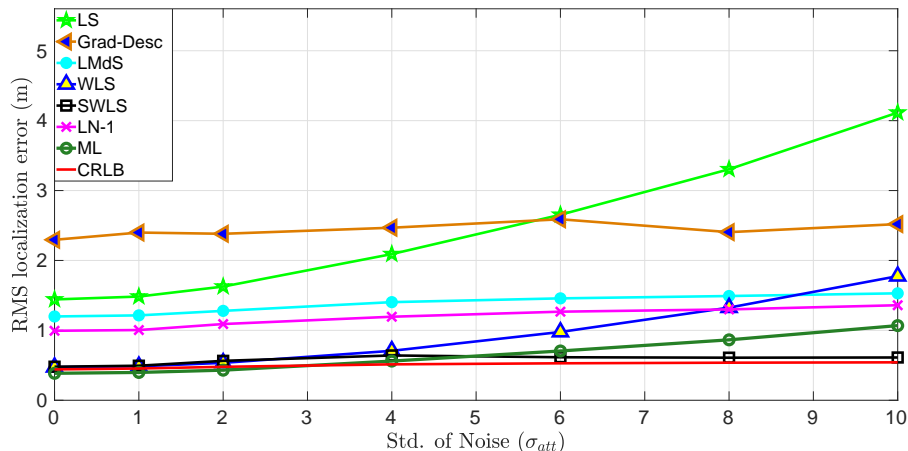
Next we study the performance of the localization techniques as the malicious anchor nodes



(a) Network topology for an uncoordinated attack with randomly placed anchors nodes (Percentage of malicious anchor nodes is 28%).



(b) RMS localization error of the secure localization techniques with $\sigma = 2$ dB as a function of σ_{att} .

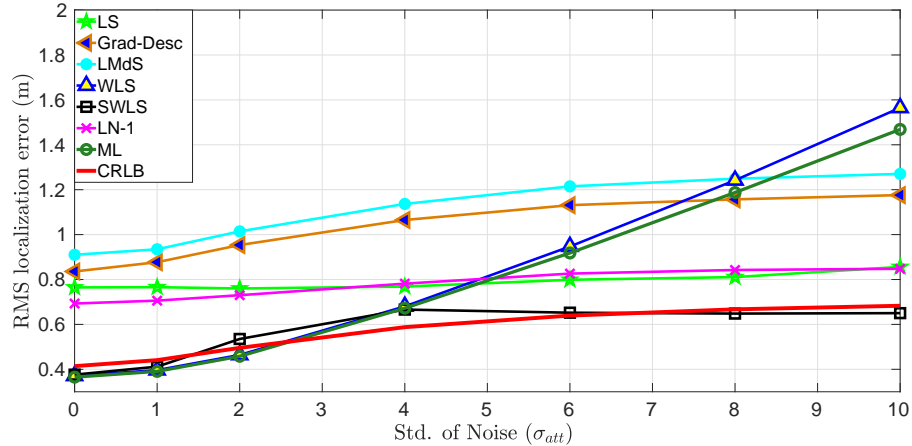


(c) RMS localization error as a function of σ_{att} with $\sigma = 2$ dB and the target node at location (10,60).

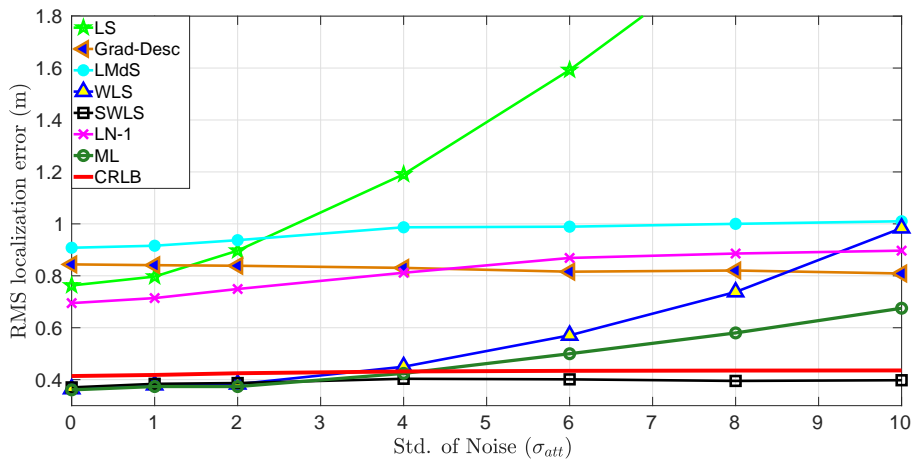
Fig. 4: Performance of secure localization techniques under uncoordinated attack with random uniformly distributed anchor nodes and $P = 10$ packets.

are moved from the center towards the edge of the network. The network topology and the percentage of anchor nodes are kept the same as in Fig. 4. The target node is at the center of the network and two scenarios are considered with malicious anchors located: (i) within 32 m of the target node, and (ii) more than 45 m from the target node. The localization performance for these scenarios are shown in Fig. 5(a) and Fig. 5(b). It is observed that LS is significantly affected by the position of the malicious anchor nodes and its performance deteriorates as the malicious anchor nodes move towards the edge of the network. It is also observed from Fig. 5(a) that LS outperforms LMdS and Grad-Desc when malicious anchor nodes are located close to the target. LS gives equal weight to measurements from all the anchor nodes, and from Lemma IV.3 we know that distance estimates for the anchor nodes located farther from the target node tend to have large errors due to σ_{att} .

In Fig. 5(a), we see that the localization performance of LMdS and Grad-Desc deteriorates gradually with increase in the value of σ_{att} . However, as the malicious anchor nodes move away from the target node and towards the edge of the network, these two techniques display robustness to the attack. LMdS and Grad-Desc pick four and $\frac{N}{2}$ anchor nodes, respectively. In Fig. 5(a), as the malicious anchor nodes are close to the target node, the residuals of the subset in LMdS or their gradients in Grad-Desc are lower than when the malicious anchor nodes are farther from the target nodes resulting in some malicious anchor nodes getting picked. In contrast



(a) RMS localization error when the malicious anchor nodes are close to the target node (within 32 m).



(b) RMS localization error when the malicious anchor nodes are located at the edge of the network.

Fig. 5: Localization performance under uncoordinated attack when the malicious anchor nodes are moved from the center to the edge of the network. ($\sigma = 2$ dB, $P = 10$ packets, and percentage of malicious anchor is 28%.)

to LS, WLS is more robust as the malicious anchor nodes move towards the edge of the network, because it assigns large weight to the anchor nodes that are located close to the target node.

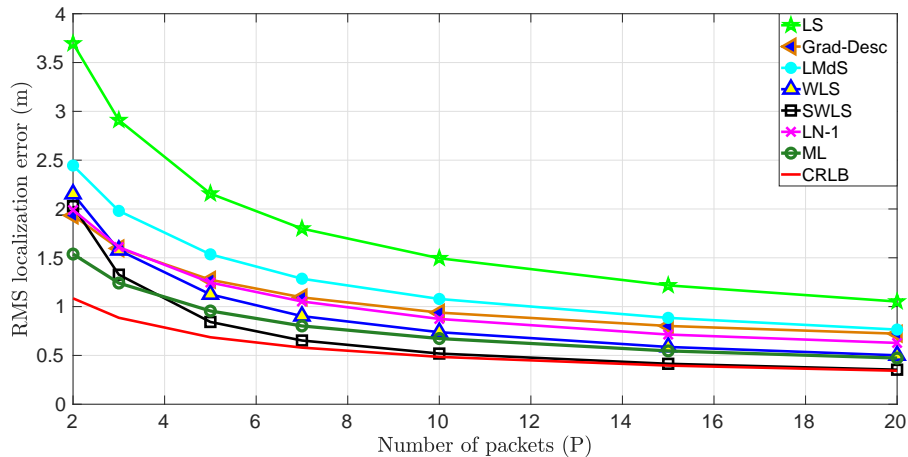
SWLS outperforms the other techniques in the scenarios shown in Fig. 5. In Fig. 5(a), SWLS results in an abrupt increase in the RMS localization error as σ_{att} becomes greater than σ . For $\sigma_{att} < \sigma$, σ_{eff} is almost equal to or slightly greater than σ and the localization accuracy is not significantly affected. When $\sigma_{att} > \sigma$, SWLS can identify the malicious anchor nodes and eliminate them. However when $\sigma_{att} \approx \sigma$, SWLS fails to identify the malicious anchor nodes resulting in a larger localization error as seen in Fig. 5(a). Similar behaviour is expected in

Fig. 5(b) except now the malicious anchor nodes are farther from the target and are assigned lower weights. Thus, the localization performance does not deteriorate as in Fig. 5(a). ML outperforms WLS for higher values of σ_{att} , otherwise exhibits similar trend as WLS. SWLS performance in Fig. 5 is close to the CRLB and SWLS outperforms the other estimators.

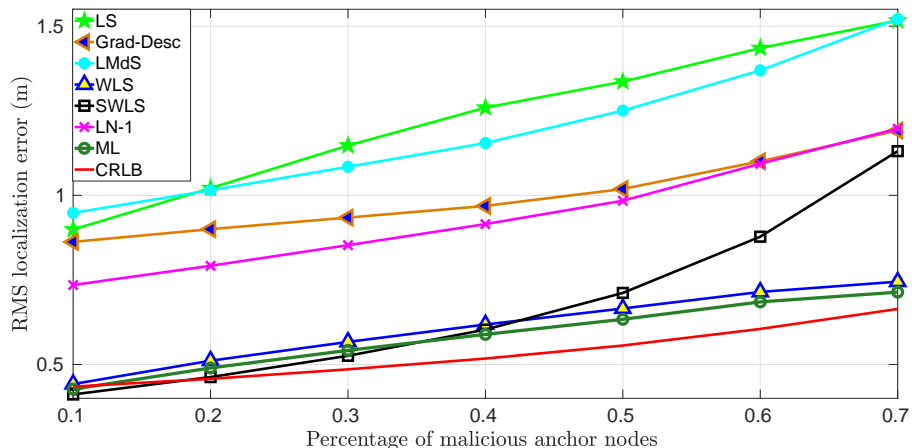
The localization performance of LN-1 is not affected by the position of the malicious anchor nodes. LN-1 performance is similar in all cases considered in Fig. 5 as well as in the case where the malicious anchor nodes are randomly placed (refer Fig. 4(b)). LN-1 does not weight the anchor nodes differently based on the position nor eliminates any anchor nodes from the localization process. It reduces the weight of those measurements that exhibit higher variance (outliers) and thus its localization performance is affected by σ_{att} and σ .

Fig. 6 shows the result of simulations carried out to understand the effect of the number of packets (P) and the percentage of malicious anchor nodes on the localization performance. The network topology is the same as in Fig. 4(a). Fig. 6(a) shows that with $P = 2$, LN-1 and Grad-Desc outperform WLS and SWLS, however as P increases WLS and SWLS outperform the other techniques. As P increases, the estimated distances become more accurate resulting in a better estimate of the variance of d^2 (refer (10)), and thus the performance of WLS and SWLS improves at a faster rate than the other techniques (except LS). For $P > 10$, the RMS localization error of WLS and SWLS is close to ML and CRLB, respectively.

In Fig. 6(b), the localization performance of all the techniques is found to deteriorate as the percentage of malicious anchor nodes increases. From (18), as $\text{card}(\mathcal{A}_m)$ increases (and $\text{card}(\mathcal{A}_{nm})$ decreases), the individual elements of the Fisher matrix \mathbf{F}_{uc} decrease since $\sigma_{\text{eff}} > \sigma$. Thus the overall CRLB also increases with the number of malicious anchor nodes in the system. The performance of Grad-Desc, LN-1, LMdS, and SWLS begins to deteriorate at a faster rate when the percentage of malicious anchor nodes exceeds 50%. In this scenario, SWLS is able to eliminate the malicious anchor nodes and computes the target node position using the remaining non-malicious anchor nodes. The performance deteriorates due to the relatively fewer anchor nodes. LMdS estimates the target node position using a subset of four anchor nodes, and as the percentage of malicious anchor nodes increases, the chances of LMdS picking one or more malicious anchor nodes in its final subset also increase.



(a) RMS localization error as a function of the number of received packets (P) ($\sigma = 2$ dB, $\sigma_{\text{att}} = 6$ dB, and 28% of the anchor nodes are malicious).

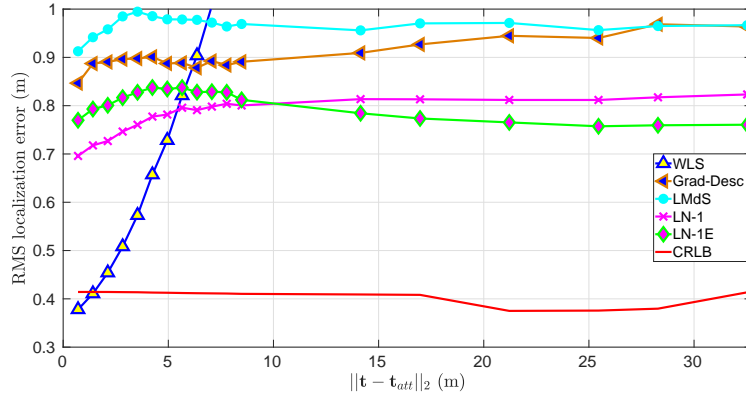


(b) RMS localization error as a function of the percentage of malicious anchor nodes ($\sigma = 2$ dB, $\sigma_{\text{att}} = 4$ dB, and $P = 10$ packets).

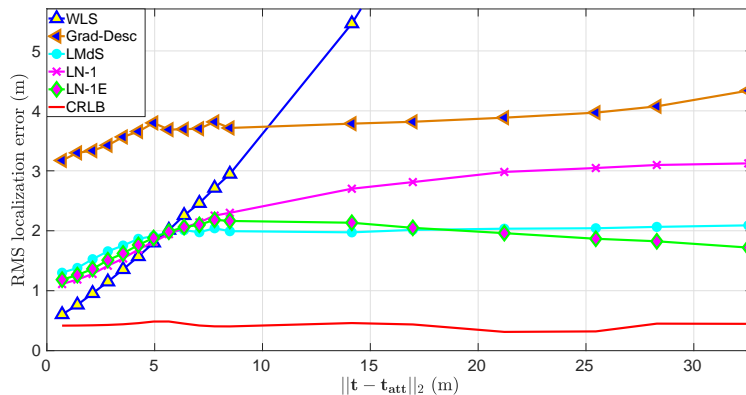
Fig. 6: Performance of secure localization techniques as a function of the number of received packets and percentage of malicious anchors in uncoordinated attack.

B. Coordinated attack

For coordinated attack, we consider the following localization techniques: WLS, Grad-Desc, LMdS, LN-1, and LN-1E. The other techniques result in poor localization performance under coordinated attack. SWLS does not perform well as it attempts to differentiate malicious anchor nodes from non-malicious ones based on the variation in the received power. This strategy fails as the malicious anchor nodes maintain a fixed transmit power in coordinated attack. Thus, we have not considered SWLS technique for the coordinated attack scenario. Fig. 7 presents the



(a) RMS localization error when 10% of anchor nodes are malicious.



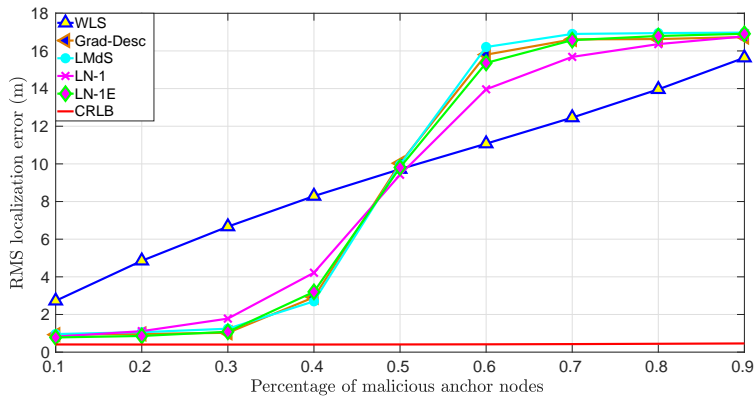
(b) RMS localization error when 28% of anchor nodes are malicious with the target node at location (5,50).

Fig. 7: Performance of secure localization techniques in coordinated attack scenario ($\sigma = 2$ dB and $P = 10$ packets).

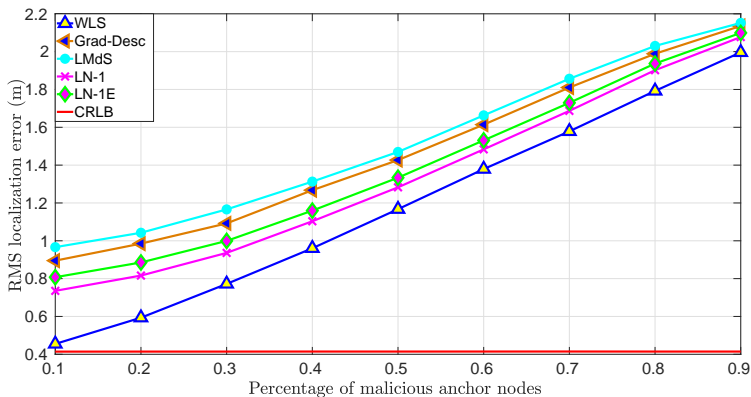
localization performance for a coordinated attack scenario as the distance between \mathbf{t} and \mathbf{t}_{att} is increased. The network topology is the same as in Fig. 4(a).

In Fig. 7(a), with 10% malicious anchor nodes, WLS significantly outperforms the other techniques when the coordinated attack is mild. However, as the attack becomes stronger the WLS performance deteriorates rapidly. LN-1 and LN-1E result in similar performance and both outperform LMdS and Grad-Desc. The poor performance of LMdS and Grad-Desc is due to the elimination of certain anchor nodes from the localization process. When the percentage of malicious anchor nodes is low and \mathbf{t}_{att} is close to \mathbf{t} , eliminating the malicious anchor nodes does not improve the localization accuracy as the measurement noise tends to determine the localization performance.

In Fig. 7(b), we show the performance of the localization techniques as the target node moves



(a) RMS localization error with $\mathbf{t}_{\text{att}} = [t^x + 12 \ t^y + 12]^T$ and $\|\mathbf{t} - \mathbf{t}_{\text{att}}\|_2 = 16.97$ m.



(b) RMS localization error with $\mathbf{t}_{\text{att}} = [t^x + 1.5 \ t^y + 1.5]^T$ and $\|\mathbf{t} - \mathbf{t}_{\text{att}}\|_2 = 2.12$ m.

Fig. 8: Performance of the secure localization techniques in a coordinated attack as a function of the percentage of malicious anchor nodes ($\sigma = 2$ dB and $P = 10$ packets).

closer to the edge of the network. The performance of Grad-Desc degrades significantly, while the performance of LN-1E and LMdS are similar and degrade to a lesser extent. From (19), it is noted that the FIM \mathbf{F}_c does not directly depend on $\|\mathbf{t} - \mathbf{t}_{\text{att}}\|_2$, and thus the CRLB in Fig. 7 is almost constant. It is also observed that Grad-Desc, LMdS, LN-1, and LN-1E follow a similar trend as the CRLB.

In Fig. 8, we study the localization performance under a coordinated attack as a function of the percentage of malicious anchor nodes. This has been simulated for two different values of \mathbf{t}_{att} representing mild and severe forms of the attack. In Fig. 8(a), it is seen that Grad-Desc, LMdS, LN-1, and LN-1E outperform WLS when the percentage of malicious anchor nodes is less than 50%. However, as the percentage of malicious anchor nodes goes above 50% WLS outperforms the other techniques. Grad-Desc retains 50% of the anchor nodes, and as

the percentage of malicious anchor nodes exceeds 50%, it ends up using measurements from malicious nodes for localization. LMdS also fails to consistently find a subset containing only non-malicious anchor nodes. For LN-1 and LN-1E, the number of outliers increases with the increase in the percentage of malicious anchor nodes. This affects the robustness of ℓ_1 -norm optimization as the measurements from the malicious anchor nodes are assigned the same weight as measurements from non-malicious anchor nodes. Unlike Grad-Desc, LMdS, and LN-1E, LN-1 does not attempt to classify or cluster the measurements and instead it fits a continuous function to the measurements. Thus, when the percentage of malicious anchor nodes exceeds 50%, LN-1 achieves better performance than Grad-Desc, LMdS, and LN-1E.

In Fig. 8(b), we consider a milder form of the coordinated attack where the malicious anchor nodes attempt to make the target node appear at $(t^x + 1.5, t^y + 1.5)$ instead of its true location (t^x, t^y) . In this case, WLS outperforms the other techniques and it is followed by LN-1 and LN-1E. The performance of Grad-Desc, LMdS, and LN-1E is comparatively poor due to their anchor elimination process. From the CRLB expression for a coordinated attack (19), it is seen that as the percentage of malicious anchor nodes increases, $\text{card}(\mathcal{A}_m)$ increases and at the same time $\text{card}(\mathcal{A}_{nm})$ decreases, such that the CRLB remains almost constant.

C. Computational Complexity

We next present a comparison of the computational complexity of the different localization techniques. Table II shows the asymptotic complexities of the secure localization techniques considered in this work. For WLS, line 5 of Algorithm 1 is the dominant computational step. Computing $\hat{\mathbf{q}}$ requires five matrix multiplications and one matrix inversion. Therefore, the computational complexity of WLS is given by $\mathcal{O}(3N^2 + 9N + 3N + 3^3 + 3^2 + N^2) \simeq \mathcal{O}(N^2)$. Similarly, the computational complexity of LS is $\mathcal{O}(N^2)$ and SWLS is $\mathcal{O}((\text{card}(\mathcal{M}))^2)$, where \mathcal{M} is the set of non-malicious anchor nodes identified by SWLS. LN-1 executes (16a), (16b), and (16c) in an iterative manner until convergence is achieved. Assuming ADMM requires k_{ADMM} iterations on average to converge, and the computational complexity of (16a) is $\mathcal{O}(N)$, the computational complexity for the ADMM steps is $\mathcal{O}(k_{\text{ADMM}}N)$. Thus, the computational complexity of LN-1 is $\mathcal{O}(\max(k_{\text{ADMM}}N, N^2)) \simeq \mathcal{O}(k_{\text{ADMM}}N)$, as $k_{\text{ADMM}} > N$ in general. In addition to the steps in LN-1, LN-1E involves K-means clustering which has a complexity of $\mathcal{O}(NTk_{\text{K-means}})$ [45], where $k_{\text{K-means}}$ is the number of average iterations and T is the complexity for calculating the distance between two data points. The computational complexity of LN-1E

TABLE II

Computational complexity of the different localization techniques.

| LS | WLS | SWLS | LN-1 | LN-1E | Grad-Desc | LMdS |
|--------------------|-----|---|---------------------------------|---|-------------------------------|-----------------------------------|
| $\mathcal{O}(N^2)$ | | $\mathcal{O}(\text{card}(\mathcal{M})^2)$ | $\mathcal{O}(k_{\text{ADMM}}N)$ | $\mathcal{O}(\max(NTk_{\text{K-means}}, k_{\text{ADMM}}N))$ | $\mathcal{O}(k_{\text{GD}}N)$ | $\mathcal{O}(M_{\text{LMdS}}N^2)$ |

is $\mathcal{O}(\max(NTk_{\text{K-means}}, k_{\text{ADMM}}N))$. LMdS algorithm involves two main operations: (i) dividing the RSSI measurements into M_{LMdS} subsets with each subset consisting of N_{LMdS} anchor nodes, and the target location is estimated for each subset using LS technique, and (ii) computing median of the residue of the results obtained from each of the subsets. The computational complexity of the first operation is $\mathcal{O}(M_{\text{LMdS}}N_{\text{LMdS}}^2)$ and the second operation is $\mathcal{O}(M_{\text{LMdS}}N^2)$. Since $N > N_{\text{LMdS}}$ in general, LMdS has a computational complexity of $\mathcal{O}(M_{\text{LMdS}}N^2)$. The computational complexity of Grad-Desc is $\mathcal{O}(k_{\text{GD}}N)$ where k_{GD} is the total number of iterations. From Table II it can be observed that the computational complexity of LN-1, LN-1E, and Grad-Desc varies linearly with the number of anchor nodes in the network.

VII. CONCLUSION

In this paper, we presented localization techniques that are robust in the presence of malicious anchor nodes in the network. We proposed four secure localization techniques WLS, SWLS, LN-1, and LN-1E, and compared their performance with the existing techniques Grad-Desc and LMdS. Two types of attacks were considered: uncoordinated and coordinated. All nodes in the network are assumed to transmit at a fixed power level which is known to the target node. The localization attacks are executed by the malicious anchor nodes by changing their transmit power and not reporting it to the target node. For uncoordinated attacks, the localization performance was studied with variation in the transmit power of the malicious anchor nodes, location of the malicious anchor nodes (close or far from the target node), number of packets P , and percentage of malicious anchor nodes in the network. SWLS outperformed all the other techniques and was close to the CRLB in most cases. The performance of WLS was found to deteriorate for $\sigma_{\text{att}} > \sigma$ or when many malicious anchor nodes are located close to the target node. On the other hand, LN-1 is neither affected by an increase in σ_{att} nor by a change in the locations of the malicious anchor nodes. For coordinated attacks, the localization performance was studied as a function of the severity of the attack in terms of the distance between the actual and reported locations of the target node and variation in the percentage of malicious anchor nodes. LN-1 and LN-1E

perform better than the other techniques with lower percentage of malicious anchor nodes and under milder form of the coordinated attack. WLS outperforms all other techniques when the attack is mild or the percentage of malicious anchor nodes exceeds 50%. The computational complexity of LN-1 and LN-1E varies linearly with the number of anchor nodes in the network.

APPENDIX A

PROOF OF (13)

Let $l(\sigma_{\text{est}}) \triangleq v - f_d^{\text{var}}(\bar{d}_i, \sigma_{\text{est}})$ where $v = \text{Var}(d_{i1}, d_{i2}, \dots, d_{iP})$. It can be shown that:

$$\frac{\partial^2 f_{d_i}^{\text{Var}}(\bar{d}_i, \sigma_{\text{est}})}{\partial \sigma_{\text{est}}^2} = \underbrace{\frac{2\bar{d}_i^2}{18.86n^2} \exp\left(\frac{\sigma_{\text{est}}^2}{18.86n^2}\right)}_{k_1} \left[\underbrace{2 \exp\left(\frac{\sigma_{\text{est}}^2}{18.86n^2}\right)}_{k_2} \underbrace{\left(1 + \frac{4\sigma_{\text{est}}^2}{18.86n^2}\right)}_{k_3} - \underbrace{\left(1 + \frac{2\sigma_{\text{est}}^2}{18.86n^2}\right)}_{k_4} \right]$$

where $k_2 k_3 - k_4$ is always positive because $k_3 \geq k_4$ and $k_2 \geq 2$. So, $\frac{\partial^2 f_{d_i}^{\text{Var}}(\bar{d}_i, \sigma_{\text{est}})}{\partial \sigma_{\text{est}}^2} \geq 0$ and $f_{d_i}^{\text{Var}}(\bar{d}_i, \sigma_{\text{est}})$ is a convex function. Therefore, $l(\sigma_{\text{est}})$ is a concave function.

Remark. If function $f: \mathbb{R}_0^+ \rightarrow \mathbb{R}$ is even, concave, $f(x=0) \geq 0$, and $\exists \epsilon (\geq 0)$ such that $f(x) \leq \epsilon$ then $x^* = \arg \min_{x \geq 0} |f(x)| \implies f(x^*) = 0$.

Using the above remark, optimal value ($\hat{\sigma}_{\text{est}}$) of the optimization problem in line 5 of Algorithm 2 can be obtained by solving $l(\hat{\sigma}_{\text{est}}) = 0$ as $l(\sigma_{\text{est}})$ is concave, even function with $l(\sigma_{\text{est}} = 0) = v$ as $f_d^{\text{var}}(\bar{d}_i, \sigma_{\text{est}} = 0) = 0$, and is upper bounded by a non-negative constant ($l(\sigma_{\text{est}}) \leq v$, as $f_d^{\text{var}}(\bar{d}_i, \sigma_{\text{est}}) \geq 0$). The objective function of the optimization problem under consideration i.e., $|l(\sigma_{\text{est}})|$ is neither convex nor concave when $\sigma_{\text{est}} \geq 0$ as $|l(\sigma_{\text{est}})|$ is concave when $\sigma_{\text{est}} \in [0, \hat{\sigma}_{\text{est}}]$ and convex when $\sigma_{\text{est}} \in [\hat{\sigma}_{\text{est}}, \infty)$.

REFERENCES

- [1] J. Jiang, G. Wang, and K. C. Ho, "Sensor network-based rigid body localization via semi-definite relaxation using arrival time and doppler measurements," *IEEE Trans. Wireless Commun.*, vol. 18, no. 2, pp. 1011–1025, Feb. 2019.
- [2] S. Salari, I. Kim, and F. Chan, "Distributed cooperative localization for mobile wireless sensor networks," *IEEE Wireless Commun. Lett.*, vol. 7, no. 1, pp. 18–21, Feb. 2018.
- [3] Z. Wang, H. Zhang, T. Lu, and T. A. Gulliver, "Cooperative rssi-based localization in wireless sensor networks using relative error estimation and semidefinite programming," *IEEE Trans. Veh. Technol.*, vol. 68, no. 1, pp. 483–497, Jan. 2019.
- [4] S. Srirangarajan and D. Pesch, "Source localization using graph-based optimization technique," in *IEEE Wireless Commun. and Netw. Conf. (WCNC)*, Apr. 2013, pp. 1127–1132.
- [5] Z. Shen, S. Cao, W.-X. Wang, Z. Di, and H. E. Stanley, "Locating the source of diffusion in complex networks by time-reversal backward spreading," *Physical Review E*, vol. 93, no. 3, pp. 1–9, Mar. 2016.

- [6] W. H. Lee, J. Choi, J. H. Lee, Y. H. Kim, and S. C. Kim, "Distributed power control-based connectivity reconstruction game in wireless localization," *IEEE Commun. Lett.*, vol. 21, no. 2, pp. 334–337, Feb. 2017.
- [7] S. M. Kay, *Fundamentals of statistical signal processing*. Prentice Hall PTR, 1993.
- [8] T. Rappaport, *Wireless Communications: Principles and Practice*, 2nd ed. Upper Saddle River, NJ, USA: Prentice Hall PTR, 2001.
- [9] B. Jang and H. Kim, "Indoor positioning technologies without offline fingerprinting map: A survey," *IEEE Commun. Surveys Tuts.*, vol. 21, no. 1, pp. 508–525, Firstquarter 2019.
- [10] A. Yassin, Y. Nasser, M. Awad, A. Al-Dubai, R. Liu, C. Yuen, R. Raulefs, and E. Aboutanios, "Recent advances in indoor localization: A survey on theoretical approaches and applications," *IEEE Commun. Surveys Tuts.*, vol. 19, no. 2, pp. 1327–1346, Second quarter 2017.
- [11] B. Mukhopadhyay, S. Sarangi, and S. Kar, "Performance evaluation of localization techniques in wireless sensor networks using RSSI and LQI," in *Nat. Conf. Commun. (NCC)*, Feb. 2015, pp. 1–6.
- [12] S. Srirangarajan, A. H. Tewfik, and Z. Q. Luo, "Distributed sensor network localization using SOCP relaxation," *IEEE Trans. Wireless Commun.*, vol. 7, no. 12, pp. 4886–4895, Dec. 2008.
- [13] I. Guvenc and C. C. Chong, "A survey on TOA based wireless localization and NLOS mitigation techniques," *Commun. Surveys Tuts.*, vol. 11, no. 3, pp. 107–124, 3rd Quarter 2009.
- [14] J.-R. Jiang, C.-M. Lin, F.-Y. Lin, and S.-T. Huang, "ALRD: AoA localization with RSSI differences of directional antennas for wireless sensor networks," in *Int. Conf. Inf. Society (i-Society)*, Jun. 2012, pp. 304–309.
- [15] T. He, C. Huang, B. M. Blum, J. A. Stankovic, and T. Abdelzaher, "Range-free localization schemes for large scale sensor networks," in *Proc. Int. Conf. Mobile Computing and Netw. (MobiCom)*, Sep. 2003, pp. 81–95.
- [16] R. Stoleru, T. He, and J. A. Stankovic, "Range-free localization," in *Secure Localization and Time Synchronization for Wireless Sensor and Ad Hoc Networks*. Springer US, 2007, pp. 3–31.
- [17] P. Sikka, P. Corke, P. Valencia, C. Crossman, D. Swain, and G. Bishop-Hurley, "Wireless ad hoc sensor and actuator networks on the farm," in *Proc. 5th Int. Conf. Inf. Processing Sensor Netw. (IPSN)*, Apr. 2006, pp. 492–499.
- [18] Y. C. Wang and G. W. Chen, "Efficient data gathering and estimation for metropolitan air quality monitoring by using vehicular sensor networks," *IEEE Trans. Veh. Technol.*, vol. 66, no. 8, pp. 7234–7248, Aug. 2017.
- [19] C. Costa, F. Antonucci, F. Pallottino, J. Aguzzi, D. Sarriá, and P. Menesatti, "A review on agri-food supply chain traceability by means of RFID technology," *Food and Bioprocess Technology*, vol. 6, no. 2, pp. 353–366, Feb. 2013.
- [20] Y. Wang, Z. Liu, D. Wang, Y. Li, and J. Yan, "Anomaly detection and visual perception for landslide monitoring based on a heterogeneous sensor network," *IEEE Sensors J.*, vol. 17, no. 13, pp. 4248–4257, Jul. 2017.
- [21] B. Mukhopadhyay, S. Sarangi, and S. Kar, "Novel RSSI evaluation models for accurate indoor localization with sensor networks," in *Nat. Conf. Commun. (NCC)*, Feb. 2014, pp. 1–6.
- [22] X. Bao, F. Bao, S. Zhang, and L. Liu, "An improved DV-Hop localization algorithm for wireless sensor networks," in *6th Int. Conf. Wireless Commun. Netw. Mobile Comput. (WiCOM)*, Sep. 2010, pp. 1–4.
- [23] A. I. G.-T. Ferreres, B. R. Alvarez, and A. R. Garnacho, "Guaranteeing the authenticity of location information," *IEEE Pervasive Comput.*, vol. 7, no. 3, pp. 72–80, Jul. 2008.
- [24] C. A. Boano, N. Tsiftes, T. Voigt, J. Brown, and U. Roedig, "The impact of temperature on outdoor industrial sensor network applications," *IEEE Trans. Ind. Informat.*, vol. 6, no. 3, pp. 451–459, Aug. 2010.
- [25] N. Baccour, A. Koubâa, L. Mottola, M. A. Zúñiga, H. Youssef, C. A. Boano, and M. Alves, "Radio link quality estimation in wireless sensor networks: A survey," *ACM Trans. Sen. Netw.*, vol. 8, no. 4, pp. 34:1–34:33, Sep. 2012.
- [26] L. Kugler, "Why GPS spoofing is a threat to companies, countries," *Commun. ACM*, vol. 60, no. 9, pp. 18–19, Aug. 2017.

- [27] U. Bareth, "Privacy-aware and energy-efficient geofencing through reverse cellular positioning," in *8th Int. Wireless Commun. Mobile Comput. Conf. (IWCMC)*, Aug. 2012, pp. 153–158.
- [28] B. Mukhopadhyay, S. Srirangarajan, and S. Kar, "Robust range-based secure localization in wireless sensor networks," in *IEEE Global Commun. Conf. (GLOBECOM)*, Dec. 2018, pp. 1–6.
- [29] R. Garg, A. L. Varna, and M. Wu, "An efficient gradient descent approach to secure localization in resource constrained wireless sensor networks," *IEEE Trans. Inf. Forensics Security*, vol. 7, no. 2, pp. 717–730, Apr. 2012.
- [30] Z. Li, W. Trappe, Y. Zhang, and B. Nath, "Robust statistical methods for securing wireless localization in sensor networks," in *Fourth Int. Symposium Inf. Process. Sensor Netw.*, Apr. 2005, pp. 91–98.
- [31] L. Lazos and R. Poovendran, "SeRLoc: Robust localization for wireless sensor networks," *ACM Trans. Sen. Netw.*, vol. 1, no. 1, pp. 73–100, Aug. 2005.
- [32] D. Liu, P. Ning, A. Liu, C. Wang, and W. K. Du, "Attack-resistant location estimation in wireless sensor networks," *ACM Trans. Inf. Syst. Secur.*, vol. 11, no. 4, pp. 22:1–22:39, Jul. 2008.
- [33] S. Jha, S. Tripakis, S. A. Seshia, and K. Chatterjee, "Game theoretic secure localization in wireless sensor networks," in *Int. Conf. the Internet Things (IOT)*, Oct. 2014, pp. 85–90.
- [34] S. Boyd and L. Vandenberghe, *Convex optimization*. Cambridge University Press, 2004.
- [35] R. Baraniuk, M. A. Davenport, M. F. Duarte, and C. Hegde, "An introduction to compressive sensing," *Connexions e-textbook*, 2011.
- [36] S. Boyd, N. Parikh, E. Chu, B. Peleato, J. Eckstein *et al.*, "Distributed optimization and statistical learning via the alternating direction method of multipliers," *Foundations and Trends in Machine learning*, vol. 3, no. 1, pp. 1–122, Jan. 2011.
- [37] D. Han and X. Yuan, "A note on the alternating direction method of multipliers," *J. Optim. Theory Appl.*, vol. 155, no. 1, pp. 227–238, Oct. 2012.
- [38] N. Parikh, S. Boyd *et al.*, "Proximal algorithms," *Foundations and Trends in Optimization*, vol. 1, no. 3, pp. 127–239, Jan. 2014.
- [39] C. M. Bishop, *Pattern Recognition and Machine Learning (Information Science and Statistics)*. Secaucus, NJ, USA: Springer-Verlag New York, Inc., 2006.
- [40] R. W. Ouyang, A. K. S. Wong, and C. T. Lea, "Received signal strength-based wireless localization via semidefinite programming: Noncooperative and cooperative schemes," *IEEE Trans. Veh. Technol.*, vol. 59, no. 3, pp. 1307–1318, Mar. 2010.
- [41] K. Yu and Y. J. Guo, "NLOS error mitigation for mobile location estimation in wireless networks," in *IEEE 65th Vehicular Technology Conf.-Spring*, Apr. 2007, pp. 1071–1075.
- [42] R. Garg, A. L. Varna, and M. Wu, "Gradient descent approach for secure localization in resource constrained wireless sensor networks," in *IEEE Int. Conf. Acoustics, Speech and Signal Process.*, Mar. 2010, pp. 1854–1857.
- [43] X. Zhang and J. G. Andrews, "Downlink cellular network analysis with multi-slope path loss models," *IEEE Trans. Commun.*, vol. 63, no. 5, pp. 1881–1894, May 2015.
- [44] C. Broyden and W. Murray, "Quasi-newton methods," *Numerical Methods for unconstrained Optimization*, W. Murray, Ed. New York: Academic I, vol. 972, 1970.
- [45] P. I. Dalatu, "Time complexity of k-means and k-medians clustering algorithms in outliers detection," *Global Journal of Pure and Applied Mathematics*, vol. 12, no. 5, pp. 4405–4418, 2016.